Assessing the Influence of Side-Chain and Main-Chain Aromatic Benzyltrimethyl Ammonium on Anion Exchange Membranes

Xiuhua Li,*[†,‡] Guanghui Nie,[†,‡] Jinxiong Tao,[†,‡] Wenjun Wu,[†,‡] Liuchan Wang,[†,‡] and Shijun Liao[†,‡]

[†]School of Chemistry & Chemical Engineering, and [‡]The Key Laboratory of Fuel Cell Technology of Guangdong Province, South China University of Technology, Guangzhou 510641, P.R. China

Ⓢ Supporting Information

ABSTRACT: 3,3′-di(4″-methyl-phenyl)-4,4′-difluorodiphenyl sulfone (DMPDFPS), a new monomer with two pendent benzyl groups, was easily prepared by Suzuki coupling reaction in high yield. A series of side-chain type ionomers (PAES-Qs) containing pendant side-chain benzyltrimethylammonium groups, which linked to the backbone by alkaline resisting conjugated C−C bonds, were synthesized via polycondensation, bromination, followed by quaternization and alkalization. To assess the influence of side-chain and main-chain aromatic benzyltrimethylammonium on anion exchange membranes (AEMs), the main-chain type ionomers (MPAES-Qs) with the same backbone were synthesized following the similar procedure. GPC and ^{1}H NMR results indicate that the bromination shows no reaction selectivity of polymer configurations and ionizations of the side-chain type polymers display higher conversions than that of the main-chain type ones do. These two kinds of AEMs were evaluated in terms of ion exchange capacity (IEC), water uptake, swelling ratio, λ, volumetric ion exchange capacity (IEC$_{Vwet}$), hydroxide conductivity, mechanical and thermal properties, and chemical stability, respectively. The side-chain type structure endows AEMs with lower water uptake, swelling ratio and λ, higher IEC$_{Vwet}$, much higher hydroxide conductivity, more robust dimensional stability, mechanical and thermal properties, and higher stability in hot alkaline solution. The side-chain type cationic groups containing molecular configurations have the distinction of being practical AEMs and membrane electrode assemblies of AEMFCs.

KEYWORDS: side-chain quaternary ammonium, Suzuki coupling reaction, bromination, alkaline anion exchange membrane, poly(arylene ether sulfone)s
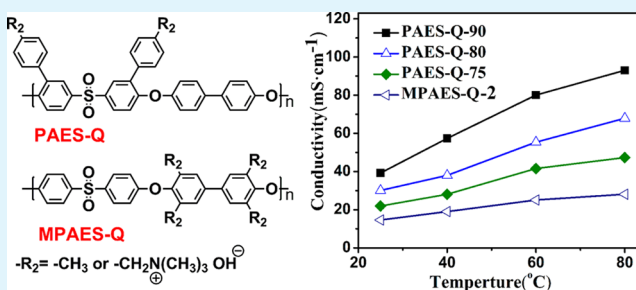
1. INTRODUCTION

Anion exchange membrane fuel cells (AEMFCs) have aroused wide concern since they overcome many of the hurdles, which must be faced in the development of liquid-electrolyte alkaline fuel cells and proton exchange membrane fuel cells (PEMFCs). Employing a solid-polymer electrolyte without mobile cations can alleviate the negative effects of CO_2 and minimize the leakage and corrosion of the liquid-electrolyte. AEMFCs can also mitigate the demand for noble metal based catalysts owing to the fast electrokinetics under basic circumstance, and lower the crossover of fuels due to the opposite direction of electroosmotic drag.[1−4] Anion exchange membrane (AEM), one of the key components of AEMFCs, separates the fuel from the oxidant and transfer anions from cathode to anode. A key challenge for AEMs in the practical application in AEMFCs is meeting the comprehensive requirements of high hydroxide anion conductivity, robust mechanical properties and good chemical stability in alkaline environment.[5] Much effort has been spent in developing better AEM materials because state-of-the-art AEMs cannot satisfy the requirements of AEMFCs. Three types of AEMs, which are classified by the function of membrane compositions, have been reported. They include alkali doped polymer membranes,[6−8] polymer/inorganic-filler

hybrid membranes,[9−11] pure polymeric membranes.[12−16] It should be pointed out that the anion conductive polymers control the comprehensive properties of AEMs except for alkali doped polymer AEMs. Especially, the chemical and thermal stabilities of the conductive polymers strongly depend on the nature of the functional group capable of transporting the hydroxyl anions (i.e. cationic groups bearing a hydroxyl counter-anion), but also the nature of the backbone.[2]

Scientists have designed new kinds of AEMs by changing the chemistry of the polymers and functionalization techniques, and the processing of the membranes. High stable backbones have been constructed from high performance engineering plastics, such as poly(arylene ether sulfone),[9,12−14,17−20] poly(arylene ether ketone),[21,22] poly(phenylene oxide),[23,24] poly(fluorenyl ether ketone sulfone),[25] and poly(ether-imide).[26] Currently, block-polymerization has been used to enhance hydroxide conductivity, mechanical and chemical stabilities of AEMs by improving phase separation between hydrophilic and hydrophobic domains.[13,23,27−29] However, the

limitation of this technique is that mechanical properties and chemical stability of the AEMs based on the block ionomers depend on the highly swollen hydrophilic domains rather than on hydrophobic domains. Many kinds of hydroxide conductive functional groups, such as quaternized ammonium (QA),[12−15,21−23,28−30] imidazolium,[27,31,32] guandinium,[33,34] or phosphonium,[16,35] have been obtained by undergoing the Menshutkin reactions between active C−X (e.g. X = Cl, Br, and I) groups of the polymers or quaternary reagents and tertiary amine, imidazole, pentamethylguanidine, tertiary phosphine. Considering of the trade-off between the cost and the chemical stability, benzyltrimethylammonium is one of the best kinds of conductive functional groups because it can avoid Hofmann elimination owing to the absence of β hydrogen. Up to now, many of these polymeric materials have demonstrated promise and progress for AEMs and established the feasibility for alkaline membrane electrode assemblies. However, no one can reach performance approaching that of current acid−based PEMFCs. Therefore, how to maximize the functions of polymer backbones and conductive functional groups is the key issue to achieve high performance AEMs.

Interestingly, most of the published works have focused on the designs of high-performance anion exchange membranes based on main chain type ionomers bearing benzyl-type cationic groups inside the polymer backbones. The strong interaction between functional groups and the backbones results in conflictive research conclusions for the AEMs with the similar backbones. Such as, Chen's work outlined that the poly(ether ketone sulfone) backbone was not stable under strong basic conditions and elevated temperatures in their types of molecular configurations,[25] whilst the poly(ether ketone sulfone) backbones in Tanaka's[15] and our previous works[14,17] could withstand severe chemical treatments under the similar testing conditions. Side-chain type ionomers distance the cationic centers from the polymer backbones by covalent side chains and avoid the interference in functions between the polymer backbones and conductive functional groups. Recently, some AEMs bearing side-chain functional groups have been reported.[30,36−40] These membranes were based on random copolymer backbones and their IECs must be tuned to balance mechanical stabilities and conductivity. To clarify the design of molecular configurations, the comparisons among varying polymer backbones and functional groups have been made. These general comparisons can't reveal well the difference influences of side-chain type ionomers and main-chain type ionomers on AEMs.

In this work, we successfully synthesized a new difluorodiphenyl sulfone monomer with two pendent benzyl groups by Suzuki coupling reaction, which gave a chance to construct side-chain type AEMs bearing the highly stable benzyl side-chain function groups linked to backbones by conjugate C−C covalent bonds. To assess the influences of side-chain and main-chain aromatic benzyltrimethylammoniums on anion exchange membranes, the main-chain type ionomers (MPAES-Qs) with the same backbone were synthesized from 2,2′,6,6′-tetramethylbiphenol and 4,4′-difluorodiphenyl sulfone following the similar procedure of side-chain type ionomers. Both two kinds of AEMs were evaluated in terms of ion exchange capacities (IEC), water uptakes, swelling ratio, λ, volumetric ion exchange capacity (IEC$_{Vwet}$), hydroxide conductivity, mechanical and thermal properties, and chemical stability.

2. EXPERIMENTAL SECTION

2.1. Materials. 4,4′-Difluorodiphenyl sulfone (DFDPS) was purchased from TCI Inc. 4,4′-Dihydroxyldiphenyl, triphenylphosphine, and 4-tolylboronic acid were purchased from Aladdin Reagent, Shanghai, China. Palladium acetate was purchased from Accela ChemBio Co., Ltd, Shanghai. All the other solvents and regents were brought from commercial sources and were used as received. 3,3′-Dibromo-4,4′-difluorodiphenyl sulfone (DBDFDPS) was synthesized according to Li's work.[41] 2,2′,6,6′-Tetramethylbiphenol (TMBP) was synthesized according to the published work.[19]

2.2. Synthesis of 3,3′-Di(4″-methyl-phenyl)-4,4′-difluorodiphenyl Sulfone (DMPDFDPS). To a 250 mL Schlenk flask equipped with a mechanical stirrer, 5.562 g (13.5 mmol) of DBDFDPS, 4.590 g (33.75 mmol) of 4-tolylboronic acid, 11.4 g (54 mmol) of potassium phosphate, 303 mg (1.35 mmol) of palladium acetate, 708 mg (2.7 mmol) of triphenylphosphine, and 60 mL of toluene were charged. The reaction mixture was vacuumed with a circulating pump, and heated at 110 °C for 24 h. And then the solvent was removed by rotary evaporation to give crude product. The crude product was recrystallized from toluene twice to afford a pure white crystal 3,3′-di(4″-methyl-phenyl)-4,4′-difluorodiphenyl sulfone. Yield: 89%. ^{1}H NMR (400 MHz, DMSO-d_6; ppm): 8.13−8.15 (m, 4H), 7.59−7.61 (m, 2H), 7.48−7.50 (d, 4H), 7.32−7.34 (d, 4H), 2.37 (s, 6H).

2.3. Synthesis of Poly(arylene ether sulfone)s Containing Aromatic Side-Chain Benzylmethyl Groups (PAES-Me). Poly(arylene ether sulfone)s containing aromatic side-chain benzylmethyl groups were synthesized via nucleophilic substitution polycondensation. A 100 mL three-neck round-bottomed flask, equipped with a Dean-stark trap, a condenser, a nitrogen inlet/outlet, and a magnetic stirrer, was charged with DMPDFDPS (7.3865 g, 17 mmol), 4,4′-dihydroxyldiphenyl (3.1656 g, 17 mmol), potassium carbonate (3.5190 g, 25.5 mmol), DMAc (25 mL), and toluene (25 mL). The reaction was performed at 145 °C for 4 h under nitrogen atmosphere to complete dehydration. After removing toluene, the reaction temperature was increased to 180 °C and kept for about 18 h. When the reaction mixture became viscous, about 30 mL of additional DMAc was added. Then the reaction mixture was poured into 500 mL of methanol containing 4 mL of concentrated HCl. The product was washed several times with deionized water and methanol and dried at 80 °C under vacuum for 24 h to give PAES-Me with a yield of 93.5%. ^{1}H NMR (400 MHz, CDCl$_3$; ppm): 8.02-8.04 (d, 2H), 7.83−7.86 (dd, 2H), 7.49−7.53 (t, 8H), 7.24−7.26 (m, 4H), 7.02−7.07 (m, 8H), 2.39 (s, 6H). GPC: M_n 107 kg mol^{-1}, M_w 214 kg mol^{-1}, M_w/M_n = 2.0.

2.4. Synthesis of Bromomethylated Poly(arylene ether sulfone)s Containing Aromatic Side-Chain Benzylmethyl Groups (PAES-Br). The bromomethylated polymers were named as PAES-Br-x, where x represents the molar ratios of NBS to benzylmethyl groups in the repeating unit of PAES-Me. A typical procedure, for example, PAES-Br-90 was as follows. PAES-Me (0.5 g, the amount of −CH$_3$ was 1.722 mmol) and 15 mL of 1,1,2,2-tetrachloroethane were added into a three-necked flask equipped with a mechanical stirrer, a nitrogen inlet, and a condenser. Then NBS (0.2452 g, 1.3776 mmol) and AIBN (11 mg) were added to the reaction mixture. The reaction was carried out at 80 °C for 4 h to give a pale yellow mixture. The mixture was then cooled to room temperature and poured into 100 mL of methanol to precipitate out the crude brominated polymer. The precipitate was washed several times with methanol, and dried in a vacuum at 80 °C for 24 h to give PAES-Br-90 with a yield of 94.5%. ^{1}H NMR (400 MHz, CDCl$_3$; ppm): 8.01 (s, 2H), 7.82-7.90 (m, 2H), 7.41-7.63 (m, 12H), 6.98-7.079 (m, 8H), 4.50 (s, −CH$_2$Br), 2.37 (s, −CH$_3$). GPC: M_n 86 kg mol^{-1}, M_w 176 kg mol^{-1}, M_w/M_n = 2.0.

2.5. Fabrication of the Side-Chain Type AEMs Based on PAES-Qs: Membrane Preparation, Quaternization, and Alkalization. PAES-Brs (0.5 g) were dissolved in 8 mL of 1,1,2,2-tetrachloroethane, followed by casting on flat glass plates. After drying at room temperature for 24 h, light yellow and tough membranes were obtained. The membranes were immersed in 33% trimethylamine aqueous solution at room temperature for 48 h and then washed with deionized water several times. The obtained quaternized membranes

were immersed in 1 M sodium hydroxide aqueous solution for another 48 h to obtain the OH⁻ form membrane. Finally, the obtained quaternized poly(arylene ether sulfone)s (PAES-Qs) membranes were washed several times with deionized water and immersed in deionized water for 48 h to remove residual NaOH. ^{1}H NMR (400 MHz, DMSO-d_6; ppm): 7.96−8.12 (m, 4H), 7.49−7.83 (m, 12H), 7.05−7.31 (m, 8H), 4.46 (s, −CH$_2$Br), 3.06 (s, −N(CH$_3$)$_3$) 2.33 (s, −CH$_3$).

2.6. Fabrication of the Main-Chain Type AEM Based on MPAES-Qs. The main-chain type ionomers (MPAES-Qs) with the same backbone were synthesized from 2,2′,6,6′-tetramethyl-biphenol and 4,4′-difluorodiphenyl sulfone following the similar procedure of the side-chain type ionomers. The fabrication of the main chain type AEMs is shown in Scheme 2b. GPC result of MPAES-Me: M_n 65 kg mol^{-1}, M_w 111 kg mol^{-1}, M_w/M_n = 1.7. GPC result of MPAES-Br: M_n 52 kg mol^{-1}, M_w 88 kg mol^{-1}, M_w/M_n = 1.7.

2.7. Characterizations and Measurements. *2.7.1. ^{1}H NMR, TGA, GPC, and Mechanical Properties.* ^{1}H NMR spectra were obtained on a Bruker AVANCE 400S with CDCl$_3$ or DMSO-d_6 as the solvent and tetramethylsilane (TMS) as the standard. Thermogravimetric analysis (TGA) was measured with a TAINC SDT Q600 thermogravimetric analyzer under a nitrogen atmosphere, at a heating rate of 10 °C per minute from 35 to 700 °C. Gel permeation chromatography (GPC) analyses were carried out on a Waters 510 HPLC equipped with a UV detector at 254 nm (chloroform as an eluent and standard polystyrenes Shodex STANDARD SM-105 as standards). The system was operated at 25 °C with a flow of 1 mL min^{-1} solvent. The mechanical properties of membranes were evaluated using a SANS Electromechanical Universal Testing Machine (UTM6000) at a test speed of 2 mm min^{-1}. The size of the membrane sample was 50 mm × 5 mm.

2.7.2. Water Uptake and Swelling Ratio. The sample films (10 mm × 50 mm) of the AEMs were immersed into degassed deionized water under a given temperature for 24 h. Then took out the membranes and wiped the surface water away quickly with tissue paper. The fast determinations of the wet membranes offered the wet weights (W_{wet}) and wet lengths (L_{wet}). The membranes were dried at 80 °C under vacuum for 24 h to get constant weights and lengths, which were recorded as W_{dry} and L_{dry}. The water uptake (WU) and swelling ratio (SR) of the membranes were calculated by the following equations:

$$WU = \frac{W_{wet} - W_{dry}}{W_{dry}} \times 100\%$$

$$SR = \frac{L_{wet} - L_{dry}}{L_{dry}} \times 100\%$$

2.7.3. Ion Exchange Capacity (IEC), λ, and Volumetric Ion Exchange Capacity (IEC$_{Vwet}$). The IEC values of the AEMs were measured by a standard back-titration method. About 100 mg of a AEM membrane was immersed in 50 mL of HCl standard solution (0.01 M) for 24 h. Then the HCl solution mixture was titrated with standardized NaOH aqueous solution using phenolphthalein as an indicator. Finally the membrane was dried at 80 °C under vacuum for 24 h until get a constant weight. The IEC value was calculated via the following formula:

$$IEC = \frac{0.0005 - M_1 V_1}{W_{dry}}$$

where M_1 (M) and V_1 (mL) are the molarity and consumed volume of the NaOH solution used in the titration, respectively. W_{dry} (g) is the weight of the dry membrane.

The number of bonded water per ammonium group (λ) was calculated by the following equation:

$$\lambda = \frac{WU}{M_{H_2O}} \times \frac{1000}{IEC}$$

where M_{H_2O} is the molecular weight of water.

Volumetric ion exchange capacity (IEC$_{Vwet}$) of hydrated membranes was calculated from the swelling ratio and the titrated IEC via the equation:

$$IEC_{Vwet} = \frac{IEC}{\frac{1}{\rho_{polymer}}(1 + SR)^3}$$

where $\rho_{polymer}$ is the density of the dry membranes.

2.7.4. Hydroxide Conductivity Measurements. The hydroxide conductivity of the AEMs was measured at an oscillating voltage of 10 mV, frequency ranging from 1 MHz to 1 kHz using a two-electrode AC impedance method with an IviumStat frequency response analyzer. The hydroxide ion conductivity (σ) was calculated as

$$\sigma = \frac{l}{RA}$$

where l (cm) is the membrane thickness, R (Ω) is the resistance of the membrane, and A (cm^2) is the electrode area of the membrane. Before the measurements, the AEMs were hydrated in degassed deionized water at least for 24 h. All measurements were performed in a vessel filled with degassed deionized water in nitrogen atmosphere.

2.7.5. Chemical Stability Test. The long-term chemical stability of the AEMs was investigated by immersing the membranes in a 1 M NaOH solution at 60 °C for 30 days (720 h). The hydroxide ion conductivity of the treated membranes was measured at 25 °C at a certain time after the complete removal of residual NaOH. The structures of the treated AMEs were characterized by ^{1}H NMR and the variations of the characteristic signals were recorded.

3. RESULTS AND DISCUSSION

3.1. Synthesis and Characterization of Monomer and Polymers.
As shown in Scheme 1, a difluorodiphenyl sulfone

Scheme 1. Synthesis of Monomer DMPDFDPS
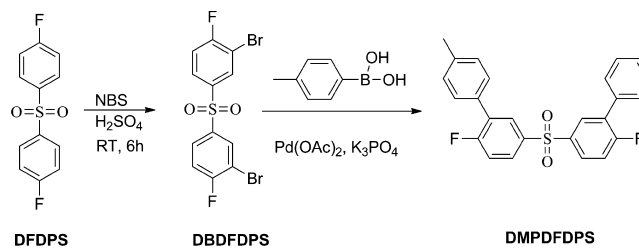
monomer with two pendent phenyl-methyl groups (DMPDFDPS) was successfully synthesized by a two-step process in a yield of 89%. The intermediate 3,3′-dibromo-4,4′-difluorodiphenyl sulfone (DBDFDPS) was synthesized by the bromination of 4,4′-difluorodiphenyl sulfone with NBS in concentrated sulfuric acid according to Li's work.[41] The final product, DMPDFDPS, was produced via Suzuki coupling reactions of DBDFDPS with 4-tolylboronic acid in the presence of palladium acetate and potassium phosphate. The structure of DMPDFDPS was identified by ^{1}H NMR analysis and shown in Figure 1. The characteristic peaks of phenyl-methyl group are observed at 2.37, 7.32, and 7.49 ppm. The signal at 2.37 ppm is contributed by the methyl group, while those signals at 7.32 and 7.49 ppm are attributed to the pendent phenyl ring.

The poly(arylene ether sulfone)s bearing side-chain aromatic benzyl-methyl quaternary ammonium groups (PAES-Qs) were synthesized by nucleophilic substitution polycondensation, bromination, quaternization and alkalization as show in Scheme 2a. GPC and ^{1}H NMR techniques were used to monitor the synthetic process. The GPC results have been attached in the experimental part. M_n and M_w of the parent polymers of side-
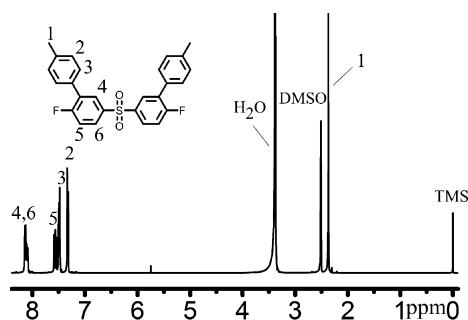
Figure 1. ^{1}H NMR spectrum of DMPDFPS.

chain type ionomers, PAES-Me and PAES-Brs, are higher than 86 and 176 kg mol^{-1} respectively. The main-chain type

ionomers (MPAES-Q) with the same backbone were synthesized from 2,2′,6,6′-tetramethyl-biphenol and 4,4′-difluorodiphenyl sulfone following the similar procedure of the side-chain type ionomers. The fabrication of the main-chain type ionomers is shown in Scheme 2b. M_n and M_w of the parent polymers of main-chain type ionomers, MPAES-Me and MPAES-Brs, are higher than 52 and 88 kg mol^{-1} respectively. The GPC results indicate that obtained ionomers, PAES-Qs and MPAES-Qs are of high molecular weights.

Figure 2 shows the ^{1}H NMR spectra of the parent polymers, PAES-Me and PAES-Br-90, and an ionomer of PAES-Q-90. The signal at 4.52 ppm in the spectrum of PAES-Br-90 (Figure 2b) was assigned to the bromomethyl groups on the side chains of PAES-Br-90. Comparing Figure 2a and b, a sharp decrease in the −CH$_3$ singlet at 2.35 ppm was observed. The degree of

Scheme 2. Synthetic Route of Poly(arylene ether sulfone)s Ionomers: (a) Side-Chain Type PAES-Qs; (b) Main-Chain Type MPAES-Qs
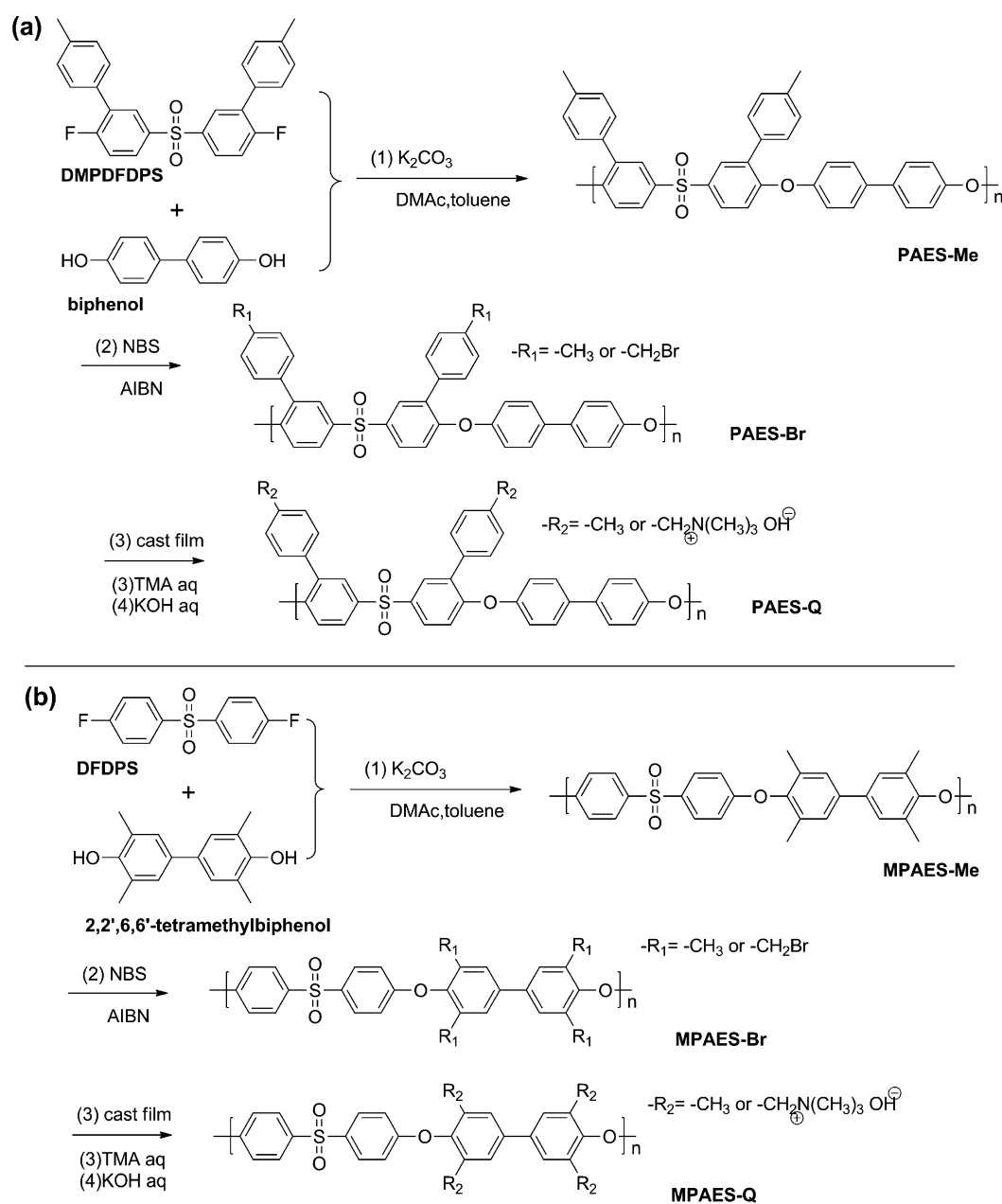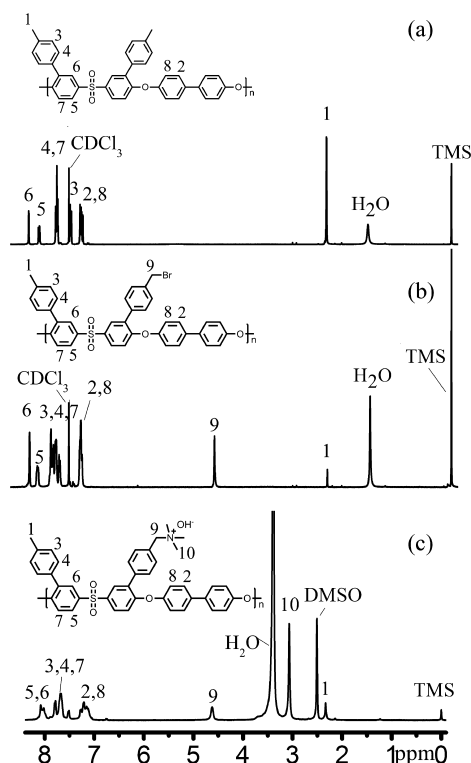
Figure 2. ^{1}H NMR spectra of (a) PAES-Me, (b) PAES-Br-90, and (c) PAES-Q-90.

bromination (DBM) is the average number of bromomethyl groups per repeating unit of PAES. DBM of PAES-Brs plays a key role in the following functionalization reactions. DBM of PAES-Brs is calculated from the integral ratio of peak **9** (4.48-4.57 ppm) belonging to methylene protons of bromomethyl groups to peak **1** (2.35 ppm) of the methyl protons (Figure 2b) using the following equation.

$$DBM = \frac{6H_9}{3H_9 + 2H_1}$$

where H_9 is the integral of brominated methyl protons, and H_1 is the integral of methyl protons. Similarly, DBM of MPAES-Brs was calculated from their ^{1}H NMR spectra. The values of DBM for PAES-Brs and MPAES-Brs are listed in Table 1. The determined values of DBM are about 88-91% of the theoretical ones, which are calculated from the molar ratios of NBS to benzylmethyl groups or methyl groups in per repeating unit of PAES-Me or MPAES-Me, respectively. There is no much difference in percent conversion between the main-chain benzylmethyl group and the side-chain benzylmethyl group.

This strongly supports the deduction that the bromination of benzylmethyl group containing PAESs is easily controlled, highly efficient and has no selectivity of the starting polymers. The ionizations of PAES-Brs and MPAES-Brs were completed by quaternization and alkalization. The results of the ionizations are tabulated in Table 1 and displayed in Figure 2c. A new signal at 3.06 ppm appears in Figure 2c, which is assigned to methyl groups in the quaternary ammonium groups. This is a direct proof of successful ionization. IEC of AEM represents the number of functional group in per unit mass of the polymer.[42] The percent conversions in the ionizations were calculated from the theoretical and experimental IEC values. Apparently the conversions of PAES-Brs are about 20 percent higher than that of MPAES-Brs. The possible reasons are that the bulky side chains in PAES-Brs benefit the establishment of loose aggregates in their membranes, and the loose aggregates favor the non-homogenous nucleophilic quaternization and ion exchange reactions. Conversely, MPAES-Brs solutions form the tight aggregates in their membranes owing to the weak stereoeffect of the methyl groups, and the tight aggregates decrease the reactivity of the non-homogenous nucleophilic quaternization and ion exchange reaction.

3.2. IEC, Water Uptake (WU), Swelling Ratio (SR), λ, Volumetric Ion Exchange Capacity (IEC$_{Vwet}$), and Hydroxide Conductivity (σ) of PAES-Qs and MPAES-Qs Membranes. Ion exchange capacity (IEC) in a scale of weight of the dry anion exchange membrane is a basic parameter of AEM and has been the most reported one.[42] All of the AEMs can be compared to clarify the effects of the designs in the scale of IEC. The IEC values of PAES-Qs varied from 1.49 to 1.68 mequiv g^{-1} with the increase of DBM, and whilst that of MPAES-Qs ranged from 1.00 to 1.30 mequiv g^{-1} (Table 1). MPAES-Brs with DBMs higher than 1.36 dissolved in trimethylamine aqueous solutions during the quaternizations and were unworthy to be discussed and compared. In the case of side-chain type ionomers, the nonpolar benzyl methylene groups between the backbone and cationic centers break the continuity of strong polar moieties and enhance the hydrophobicity of the backbone. This enables the side-chain type ionomers to have higher IECs. Table 2 lists water uptake, swelling ratio, λ, IEC$_{Vwet}$, and hydroxide conductivity of the PAES-Qs and MPAES-Qs with varying IECs. Water uptake and swelling ratio are two significant factors in conductivity performance and mechanical properties of AEM.[43] Adequate water uptake benefits the establishment and enhancement of transport channels for anions and high hydroxide conductivity of AEMs. However, excess water uptake results in deteriorations of mechanical properties, for example, excessive swelling and uncontrollable deformation. Swelling ratios of the AEMs strongly depend on the AEM materials and their water uptake.

Table 1. Results of Bromination and Ionization

membrane	DBM		conv. of bromination (%)	IEC (mequiv g^{-1})		conv of ionization (%)
	theor[a]	expt[b]		theor[c]	expt[d]	
PAES-Q-90	1.80	1.62	90	2.31	1.68 ± 0.04	73
PAES-Q-80	1.60	1.46	91	2.12	1.57 ± 0.03	74
PAES-Q-75	1.50	1.33	89	1.95	1.49 ± 0.05	76
MPAES-Q-1	1.20	1.06	88	1.98	1.00 ± 0.00	51
MPAES-Q-2	1.50	1.36	91	2.43	1.30 ± 0.00	53

[a]Theoretical DBM, calculated from feed ratios of NBS/−CH$_3$. [b]Experimental DBM, determined by ^{1}H NMR. [c]Theoretical IEC, calculated from experimental values of DBM. [d]Experimental IEC, determined by titration.

Table 2. Water Uptake, Swelling Ratio, λ, IEC$_{Vwet}$, and Hydroxide Conductivity of PAES-Qs and MPAES-Qs Membranes

membrane	IEC (mequiv g^{-1})	WU (%)		SR (%)		λ		IEC$_{Vwet}$ (mequiv cm^{-3})		σ (mS cm^{-1})	
		$T_1{}^a$	$T_2{}^b$	$T_1{}^a$	$T_2{}^b$	$T_1{}^a$	$T_2{}^b$	$T_1{}^a$	$T_2{}^b$	$T_1{}^a$	$T_2{}^b$
PAES-Q-90	1.68 ± 0.04	60.6 ± 4.1	99.5 ± 2.7	21.2 ± 3.3	33.3 ± 1.4	20.1	32.9	1.01	0.76	39.2 ± 0.2	93.0 ± 0.2
PAES-Q-80	1.57 ± 0.03	52.2 ± 2.2	80.9 ± 1.1	16.0 ± 1.9	24.1 ± 1.2	18.5	28.6	1.08	0.88	30.1 ± 0.1	67.9 ± 0.2
PAES-Q-75	1.49 ± 0.05	36.8 ± 2.1	59.6 ± 3.1	7.8 ± 0.4	15.6 ± 3.0	13.8	22.3	1.27	1.03	21.9 ± 0.1	47.3 ± 0.1
MPAES-Q-1	1.00 ± 0.00	50.1 ± 5.2	58.9 ± 2.9	12.9 ± 0.6	14.5 ± 0.2	27.5	32.4	0.74	0.71	12.6 ± 0.2	45.6 ± 0.0
MPAES-Q-2	1.30 ± 0.00	91.4 ± 1.5	424.9 ± 35.1	24.9 ± 2.0	50.0 ± 6.4	38.6	179.6	0.71	0.41	14.6 ± 0.1	28.1 ± 0.1

$^a T_1$ = 25 °C. $^b T_1$ = 80 °C.

The common tendency for these two kinds of AEMs is that water uptake and swelling ratio increase with the increases of temperature and IEC (Table 2, Figures 3 and 4). The side-
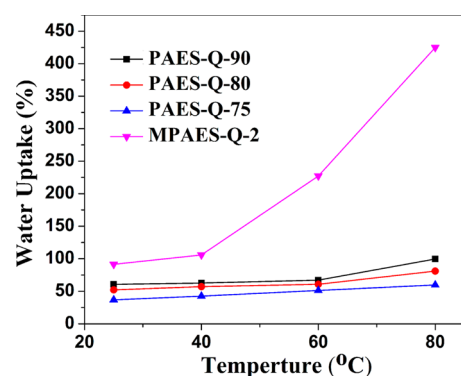

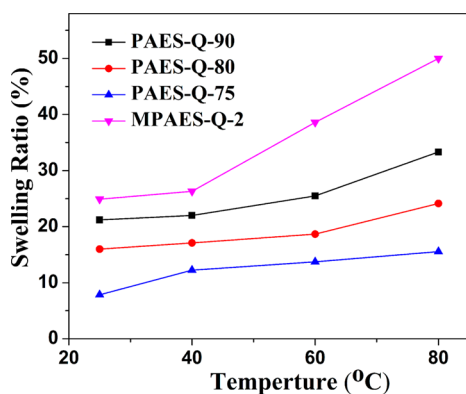**Figure 3.** Water uptake of PAES-Qs and MPAES-Qs membranes at different temperature.

Figure 4. Swelling ratio of PAES-Qs and MPAES-Qs membranes at different temperature.

chain type AEMs with higher IECs show relatively much lower water uptakes and less swelling ratios than that of the main-chain type AEMs. The temperature dependences of water uptake and swelling ratio of the main-chain type AEMs are stronger than that of the side-chain type AEMs. The MPAES-Q-2 membrane with IEC value of 1.30 mequiv g^{-1} shows the highest water uptake and swelling ratio. Actually the AEMs in AEMFCs work at water and heat circumstances. The hydroxide ions conductivity of the AEMs in AEMFCs is controlled by the active volume under given working conditions. The IECs in a scale of weight of the dry AEMs can't reflect the structures of the membranes in AEMFCs under working conditions. In convenience of exploring the relationship of hydroxide ions conductivity and the structures of the ionomers membranes,

the number of bonded water per ammonium group (λ) and volumetric ion exchange capacity (IEC$_{Vwet}$) of the hydrated ionomers membranes were calculated. IEC$_{Vwet}$ reflects the concentration of ion pairs within the ionomer matrix under hydrated (operationally relevant) conditions.[30,44] The values of IEC$_{Vwet}$ in the published works have been calculated from IECs in weight, water uptakes, and the densities of dried polymers and water assuming the additivity of volumes of water and the polymers.[30,44] These methods are problematic because the ionomers membranes are far to be ideal mixtures. IEC$_{Vwet}$ in this work is based on swelling ratio of the hydrated membranes at a given hydrated conditions and has taken account of the changes in volume with the temperature in water and IEC in weight. The common tendencies for the main-chain type and side-chain type ionomers membranes are that λ increases with the increases of temperature and IECs, and IEC$_{Vwet}$ shows adverse tendency (Table 2). λ values of main-chain type MPAES-Qs membranes are much higher than that of the side-chain type PAES-Qs membranes at the same temperatures and closing IECs. IEC$_{Vwet}$ values of MPAES-Qs membranes are much lower than that of PAES-Qs membranes at the same comparison conditions of λ. It is obvious that the functionalization technique at the terminal groups of the side chains can improve the hydrophobicity of the backbone and tune the hydrophilicity and structures of the ionomers membranes. The temperature dependences of λ and IEC$_{Vwet}$ of the main-chain type AEMs are stronger than that of the side-chain type AEMs. MPAES-Q-2 gave extremely high λ value of 179.6 and low IEC$_{Vwet}$ value of 0.41 mequiv cm^{-3}. High values of λ and IEC$_{Vwet}$ benefit the transportation of hydroxide ions. However, overly high λ results in a great decrease in IEC$_{Vwet}$, which significantly impacts the hydroxide ions conductivity of AEMs.

Adequate hydroxide conductivity is a key factor for AEMFCs to achieve high performance.[4,45] Figure 5 shows ionic conductivities of the ionomers membranes as functions of temperature. The conductivities of these two kinds of ionomers membranes increase with the increases of IEC and temperature (Figure 5 and Table 2). The side-chain type PAES-Qs membranes demonstrate much better conductivity than the main-chain type MPAES-Qs do. PAES-Q-90 gives the highest conductivity of 93.0 mS cm^{-1} at 80 °C, which is much higher than that of MPAES-Q-2 (1.30 mequiv g^{-1}, 25.1 mS cm^{-1} at 80 °C). A reasonable explanation is that the side-chain quaternary ammoniums lead effective micro-phase separation in the side-chain type AEMs, which benefits the establishment of hydroxide ion conductive channels and restricts the hydrophilicity of strong polar moieties in the backbones. Zhang et al. reported that $-CH_2-$ group of the main-chain type AEMs might be too short to induce effective micro-phase separation.[39] So do the main-chain type MPAES-Qs in this work. Large
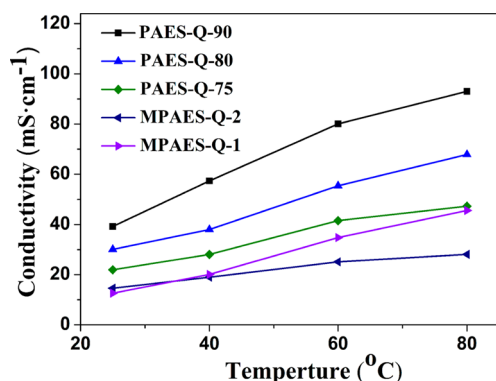
Figure 5. Ionic conductivity of PAES-Qs and MPAES-Qs membranes at different temperature.

Figure 6. Arrhenius plots of PAES-Qs and MPAES-Qs membranes.

difference in λ and IEC_{Vwet} between the PAES-Qs membranes and the MPAES-Qs membranes are the first-hand experimental proofs for the effects of the micro-phase separation.

Table 3 lists the IEC, swelling ratio, and hydroxide conductivity results of various AEMs in some of the typical published works, which are based on different polymeric materials attached with varying anion conductive groups. It is obvious that the conductivities of the PAES-Qs membranes rank among good conductive aromatic group membranes taking account of IEC, and the PAES-Qs membranes have close swelling ratios to the publish works. In the side-chain type group consisting of s-QATMA with the close IEC, the PAES-Qs membranes demonstrated the significantly improved conductivities. Compared with main-chain type group (m-QATMA)[17,19,20] and m-imidazolium,[24] the improvements of PAES-Qs are more apparent. The conductivities of PAES-Qs are even higher than some of block aromatic AEMs (B-m-QATMA) with higher IEC values.[13,28] Figure 6 displays the plots of ln σ via $1000/T$ (T is the absolute temperature) for the PAES-Qs membranes and the MPAES-Qs membranes. It is obvious that the relationship between ln σ and $1000/T$ follows Arrhenius behavior. The hydroxide transport activation energy E_a of these ionomers membranes were calculated using the following equation: $E_a = -bR$, where b is the slope of the regressed linear ln σ−$1000/T$ plots, and R is the gas constant $(8.314\ J\ (mol\ K)^{-1})$. The calculated ion transport activation
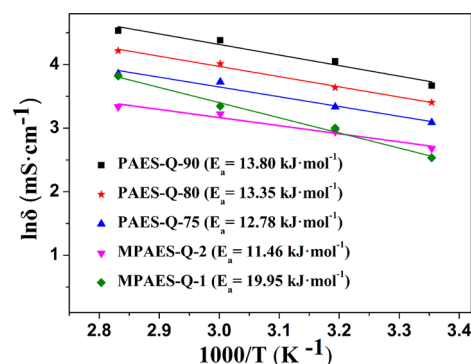
energies E_a of the PAES-Qs membranes varied from 12.78 to 13.80 kJ mol^{-1}, which are close to that of Nafion-117 (12.75 kJ mol^{-1}).[46] E_a of the MPAES-Qs membranes ranged from 11.46 to 19.95 kJ mol^{-1}. The hydroxide ion mobility in the side-chain type PAES-Qs membranes is less sensitive to temperature than that of main chain type MPAES-Q-1 membrane.

Ion transport in polymer electrolytes relies on the ion pairs concentration and the state of the ion pairs under the hydrated (operationally relevant) conditions.[44] Figure 7 shows the relationships of the conductivity via λ and IEC_{Vwet} of hydrated PAES-Qs and MPAES-Qs membranes. It is obvious that conductivity linearly grows with an increase of λ and decreases with the increasing IEC_{Vwet} in the case of the side-chain type AEMs. The possible explanations are as follows. The higher the value of λ is, the more water molecules are bonded to per ammonium group. This offers diluted solution conditions to the ion pair of ammonium and hydroxide ion and benefit the dissociation of the ion pair and the generation of free hydroxide ion. The adequate concentration of ion pairs in the hydrated membranes benefits the establishment and the continuity of ion transport channels. Excessive ion pairs inside the separate ion transport channel will suppress the dissociation of the ion pair and decrease the surface sites hopping of the hydroxide ion. In the case of the main-chain AEMs, the hydroxide conductivity increases with the increasing IEC_{Vwet} initially and then shifts down. The variation of conductivity to λ shows the similar trend taking account of the temperature. It also should be

Table 3. IEC, swell ratio and hydroxide conductivity of different AEMs reported in the literature

membrane	ionic group	IEC (mequiv g^{-1})	swell ratio (%)	conductivity (mS cm^{-1})
4(X81)[30]	s-QATMA[a]	1.74	20 °C 4, 80 °C 5	20 °C 38, 80 °C 58
PEEK-Q-100[36]	s-QATMA[a]	1.43	20 °C 15.3, 80 °C 21.2	20 °C 17, 80 °C 41
QMPAE-75[38]	s-QATMA[a]	1.35	rt 11.1, 80 °C 21.7	rt 12.3, 80 °C 30.7
OBuTMA-AAEPs-1.0[39]	s-QATMA[a]	1.75	25 °C 8.5, 60 °C 19.1	25 °C 37, 60 °C 75
M$_0$[19]	m-QATMA[b]	1.31	30 °C 15	30 °C12.8, 80 °C 58.0
QPSf[20]	m-QATMA[b]	not reported	not reported	rt 1.6
QPAE-a[17]	m-QATMA[b]	2.38	not reported	20 °C 25, 80 °C 64.7
QBPES-40[28]	B-m-QATMA[c]	1.62	20 °C 12, 60 °C 14	rt 29, 80 °C 48.0
QPAE-X15Y15[13]	B-m-QATMA[c]	1.91	20 °C 16, 60 °C 25	20 °C 20.3, 80 °C 73.6
QPE-X16Y11[29]	B-m-QATMA[c]	1.93	not reported	80 °C 144
Dim-PPO-0.22[24]	m-imidazolium[d]	1.53	35 °C 13.0	30 °C 14, 60 °C 28
Px$_7$y$_3$[18]	m-guanidinium[d]	1.21	rt 0.92 (SR in area)	30 °C 60, 80 °C 130
SCL-TPQPOH[16]	m-phosphonium[d]	1.23	60 °C 15	20 °C 38

[a]s-QATMA = side-chain type TMA based quaternary ammonium. [b]m-QATMA = main-chain type TMA based quaternary ammonium. [c]B-m-QATMA = main-chain type TMA based quaternary ammonium in block ionomers. [d]m in m-imidazolium, m-guanidinium, and m-phosphonium denotes main-chain type ionic groups.
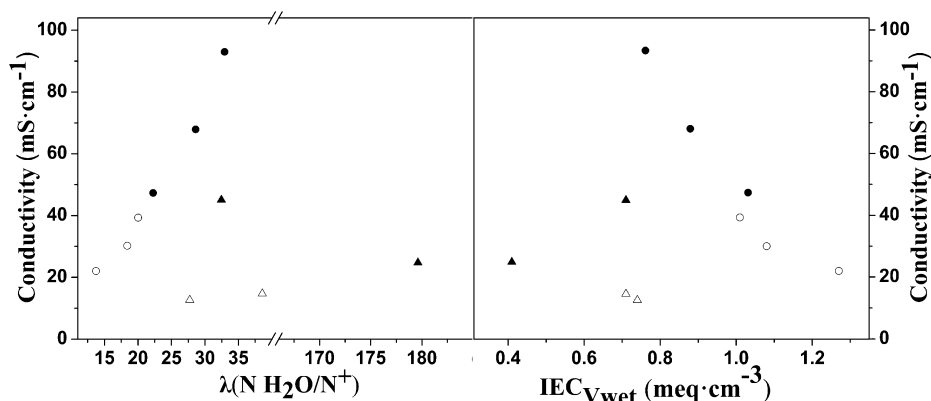
Figure 7. (a) Conductivity versus λ and (b) conductivity versus IEC_{Vwet} of the hydrated ionomers membranes. Circular symbols are for the side-chain type AEMs (PAES-Qs), and triangular symbols are for the main-chain type AEMs (MPAES-Qs). Open symbols represent values at 25 °C, and closed symbols represent values at 80 °C.

Table 4. Mechanical Properties of PAES-Qs, MPAES-Qs Membranes and Some Reported AEMs

sample	IEC (mequiv g^{-1})^a	tensile strength (MPa)^b	tensile modulus (MPa)^b	elongation at break (%)^b
PAES-Q-90	1.68 ± 0.04	15.1 ± 1.9	109.9 ± 24.1	28.3 ± 0.9
PAES-Q-80	1.57 ± 0.03	24.4 ± 0.6	356.1 ± 28.4	34.2 ± 0.8
PAES-Q-75	1.49 ± 0.05	32.0 ± 2.2	419.7 ± 50.7	15.2 ± 3.3
MPAES-Q-1	1.00 ± 0.00	14.4 ± 1.0	248.0 ± 9.2	6.2 ± 0.9
MPAES-Q-2	1.30 ± 0.00	6.9 ± 0.3	122.4 ± 3.5	6.3 ± 1.3
QMPAE-75[38]^c	1.35	17.0	not reported	20.2
OBuTMA−AAEPs-1.0[39]^c	1.75	28.0	not reported	107
Dim-PPO-0.22[24]	1.53	30.1	not reported	9.8
QBPES-40[28]^d	1.62	38.8	860	20.2
QPE-X16Y11[29]^d	1.93	13.0^e	not reported	22.0^e
Nafion-117[45]	0.91	21.1	6.6	370.6

^{a}Experimental IEC, determined by titration. ^{b}The samples were measured at 25 °C, 100% RH. ^{c}Side-chain type ionomer. ^{d}Block ionomer. ^{e}The samples were measured at 80 °C, 60% RH.

pointed out that the similar λ at high temperature give much bigger contribution to hydroxide conductivity than that at low temperature owing to the high mobility of water at high temperature. However, overly high λ results in excessively low ions concentration in the hydrated membranes, which can't build effective ion transportation channels. In conclusion, the side-chain type ionomers can afford high concentration of ion pairs and adequate λ to improve their conductivities.

3.3. Mechanical Properties and Thermal Properties. Robust mechanical and thermal properties are essential for the fabrication of membrane electrode assembly for AEMFCs. The mechanical properties of the PAES-Qs and MPAES-Qs ionomers membranes are listed in Table 4. It is clear that aromatic side-chain quaternized membranes PAES-Qs show much better mechanical properties (15.1 to 32.0 MPa) than the main chain polymers MPAES-Q-1 and MPAES-Q-2 do (6.9 to 14.4 MPa). The tensile strengths of PAES-Qs are better than that of side-chain type ionomers QMPAES-75[38] and QBuTMA-AAEPs-1.0,[39] block ionomer QPE-X16Y11 (1.93 mequiv g^{-1}),[29] and close to Dim-PPO-0.22.[24] Though PAES-Q-90 with the highest IEC of 1.68 mequiv g^{-1} has a tensile strength of 15.1 MPa less than that of Nafion -117,[44] the others two PAES-Qs membranes show much better tensile strengths. The poor mechanical properties of the main-chain MPAES-Qs are attributed to the high absorbability of water resulting from the strong coaction of the function groups and strong polar backbone. The side-chain structure breaks the field continuity of the function groups and strong polar backbone, and enlarges

the hydrophobicity of the backbone. These unique molecular configurations of side-chain type ionomers ensure good conductivity and robust mechanical properties for the corresponding AEMs.

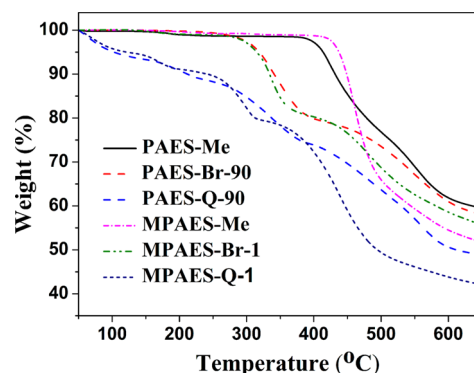Figure 8 shows the TGA curves for PAES-Me, MPAES-Me, PAES-Br-90, MPAES-Br-1, PAES-Q-90, MPAES-Q-1 from

Figure 8. TGA curves of parent polymers and ionomers.

room temperature to 700 °C. Among the first generation precursors, side-chain polymer PAES-Me commences the decomposition at temperature of 370 °C, which is a bit lower than that of main chain polymer MPAES-Me. As far as the decomposition behaviors of the second generation precursors are concerned, PAES-Br-90 and MPAES-Br-1 display the

adverse tendency to first generation precursors. Side-chain polymer PAES-Br-90 lags its decomposition behind that of the main chain polymer MPAES-Br-1. The decomposition behaviors of the ionomers, PAES-Q-90 and MPAES-Q-1, similarly demonstrate four steps processes. Combined with the results of TG-IR determination (Figure S1, Supporting Information), the first stage is attributed to absorb surface water and the second stage is assigned to the degradation of the quaternary ammonium groups. The rest third and fourth stages of weight losses were ascribed to the decompositions of the nonvolatile residual of second stage and polymer backbone, respectively. Especially the degradation of the quaternary ammonium groups of PAES-Q-90 (maximum speed of degradation at 200 °C) delays about 20 °C compared with that of MPAES-Q-1 (maximum speed of degradation at 180 °C). It is obvious that side-chain type ionomer displays much better short-term thermal stability than the main chain type ionomer does.

3.4. Long-Term Chemical Stability of Ionomers Membranes. The chemical stability of AEMs is a significant factor for the practical application of alkaline fuel cells. We evaluated the chemical stability of ionomers membranes under the conditions of 1 M NaOH solution at 60 °C. The side-chain type AEM PAES-Q-90 (1.68 mequiv g^{-1}) maintained its toughness over 30 days, whilst the main-chain type AEM MPAES-Q-1 (1.00 mequiv g^{-1}) broke into small pieces after 14 days. Figure 9 shows the declines in hydroxide conductivity at
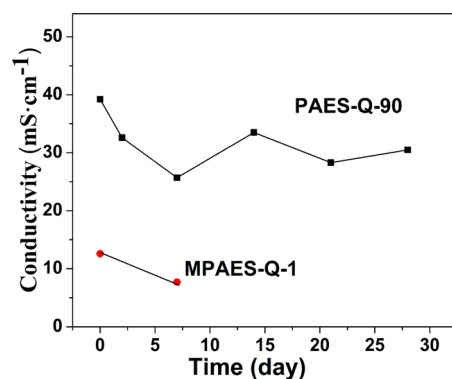

Figure 9. Hydroxide conductivity of PAES-Qs and MPAES-Qs membranes after treatment with 1 M NaOH solution at 60 °C.

25 °C of PAES-Q-90 and MPAES-Q-1 with the conditioning time. The hydroxide conductivity of the treated PAES-Q-90 at the 28th day remains at 30 mS cm^{-1}, which can satisfy the basic requirement of the hydroxide conductivity (over 10 mS cm^{-1}) for fuel cell operation.[1] The conductivity of MPAES-Q-1 decreases to 55.0% of the original value after a 7 days treatment and is disqualified to be taken the hydroxide conductivity measurement at a 14 days treatment owing to the loss of mechanical properties. The chemical structures of PAES-Q-90 before and after the stability tests were further characterized by ^{1}H NMR and displayed as Figure S2 (Supporting Information). The integral ratios of peak **9** ($-C\underline{H}_2N$), peak **10** ($-N(C\underline{H}_3)_3$) to peak **1** ($-C\underline{H}_3$, unchanged with the processing of chemical stability tests) show minor changes of less than 6% (Table S1, Supporting Information). These results revealed that the side-chain type AEM PAES-Q-90 has excellent long-term alkaline stability.

4. CONCLUSIONS

A difluorodiphenyl sulfone monomer with two pendent benzyl groups has been successfully synthesized by Suzuki coupling reaction in high yield. Combined with 4,4′-dihydroxydiphenyl, 2,2′,6,6′-tetramethyl-biphenol and 4,4′-difluorodiphenyl sulfone, two series of AEMs based on the same backbone containing side-chain type pendant benzyltrimethylammonium groups (PAES-Qs) and main-chain type benzyltrimethylammonium groups (MPAES-Qs) were precisely constructed and synthesized by nucleophilic substitution polycondensation, bromination and ionizations. GPC and ^{1}H NMR results indicated that the bromination of benzylmethyl groups containing polymers is an easy and effective way to get high active parent polymers to be ionised. The bulky side-chains in parent polymers form loose aggregates in the brominated membranes and favor the non-homogenous nucleophilic quaternization and ion exchange reactions. The tight aggregates in the brominated membranes decrease the reactivity of the functionalizations. The side-chain type AEMs PAES-Qs and the main-chain type AEMs MPAES-Qs were detailed evaluated in terms of water uptake, swelling ratio, λ, volumetric ion exchange capacity (IEC$_{Vwet}$), hydroxide conductivity, mechanical and thermal properties, and chemical stability. The side-chain type structure endows AEMs with lower water uptake, swelling ratio and λ, higher IEC$_{Vwet}$, much higher hydroxide conductivity, more robust dimensional stability, mechanical and thermal properties, and higher stability in hot alkaline solution than that of main chain type AEMs. These results confirmed that the concept to utilize side-chain type cationic groups is effective for improving the ionic conductivity of AEMs without sacrificing mechanical properties. The molecular configurations containing side-chain type cationic groups are promising as materials for practical AEMs and membrane electrode assemblies of AEMFCs.

■ ASSOCIATED CONTENT

ⓢ Supporting Information

Experimental details of TG-IR determination and ^{1}H NMR characterization, TG-IR spectra of PAES-Q-90 membrane, ^{1}H NMR spectra of the degraded PAES-Q-90 membrane, and ^{1}H-NMR integral data of the degraded PAES-Q-90 membrane. This material is available free of charge via the Internet at http://pubs.acs.org.

■ AUTHOR INFORMATION

Corresponding Author

*Tel & Fax: 8620−22236591. E-mail: lixiuhua@scut.edu.cn.

Notes

The authors declare no competing financial interest.

■ ACKNOWLEDGMENTS

■ ABBREVIATIONS

PAES-Qs, quaternized poly(arylene ether sulfone)s
AEMs, anion exchange membranes
IEC, ion exchange capacities
IEC$_{Vwet}$, volumetric ion exchange capacity
AEMFCs, exchange membrane fuel cells

PEMFCs, proton exchange membrane fuel cells
PAE-Br, bromomethylated poly(arylene ether sulfone)s

■ REFERENCES

(1) Merle, G.; Wessling, M.; Nijmeijer, K. Anion Exchange Membranes for Alkaline Fuel Cells: A Review. *J. Membr. Sci.* **2011**, *377*, 1−35.

(2) Couture, G.; Alaaeddine, A.; Boschet, F.; Ameduri, B. Polymeric Materials as Anion-Exchange Membranes for Alkaline Fuel Cells. *Prog. Polym. Sci.* **2011**, *36*, 1521−1557.

(3) Varcoe, J. R.; Slade, R. C. T. Prospects for Alkaline Anion-Exchange Membranes in Low Temperature Fuel Cells. *Fuel Cells* **2005**, *5*, 187−200.

(4) Wang, Y.; Qiao, J.; Baker, R.; Zhang, J. Alkaline Polymer Electrolyte Membranes for Fuel Cell Applications. *Chem. Soc. Rev.* **2013**, *42*, 5768−5787.

(5) Hickner, M. A.; Herring, A. M.; Coughlin, E. B. Anion Exchange Membranes: Current Status and Moving Forward. *J. Polym. Sci., Part B: Polym. Phys.* **2013**, *51*, 1727−1735.

(6) Hou, H. Y.; Sun, G. Q.; He, R. H.; Wu, Z. M.; Sun, B. Y. Alkali Doped Polybenzimidazole Membrane for High Performance Alkaline Direct Ethanol Fuel Cell. *J. Power Sources* **2008**, *182*, 95−99.

(7) Wu, G. M.; Lin, S. J.; Yang, C. C. Preparation and Characterization of PVA/PAA Membranes for Solid Polymer Electrolytes. *J. Membr. Sci.* **2006**, *275*, 127−133.

(8) Fu, J.; Qiao, J. L.; Wang, X. Z.; Ma, J. X.; Okada, T. Alkali Doped Poly(vinyl alcohol) for Potential Fuel Cell Applications. *Synth. Met.* **2010**, *160*, 193−199.

(9) Li, X.; Yu, Y.; Meng, Y. Novel Quaternized Poly(arylene ether sulfone)/Nano-ZrO$_2$ Composite Anion Exchange Membranes for Alkaline Fuel Cells. *ACS Appl. Mater. Interfaces* **2013**, *5*, 1414−1422.

(10) Wu, Y.; Luo, J.; Yao, L.; Wu, C.; Mao, F.; Xu, T. PVA/SiO$_2$ Anion Exchange Hybrid Membranes from Multisilicon Copolymers with Two Types of Molecular Weights. *J. Membr. Sci.* **2012**, *399*, 16−27.

(11) Yang, C.; Chiu, S.; Kuo, S.; Liou, T. Fabrication of Anion-Exchange Composite Membranes for Alkaline Direct Methanol Fuel Cells. *J. Power Sources* **2012**, *199*, 37−45.

(12) Yan, J.; Moore, H. D.; Hibbs, M. R.; Hickner, M. A. Synthesis and Structure−Property Relationships of Poly(sulfone)s for Anion Exchange Membranes. *J. Polym. Sci., Part B: Polym. Phys.* **2013**, *51*, 1790−1798.

(13) Li, X.; Yu, Y.; Liu, Q.; Meng, Y. Synthesis and Properties of Anion Conductive Multiblock Copolymers Containing Tetraphenyl Methane Moieties for Fuel Cell Application. *J. Membr. Sci.* **2013**, *436*, 202−212.

(14) Li, X.; Liu, Q.; Yu, Y.; Meng, Y. Quaternized Poly(arylene ether) Ionomers Containing Triphenyl Methane Groups for Alkaline Anion Exchange Membranes. *J. Mater. Chem. A* **2013**, *1*, 4324−4335.

(15) Tanaka, M.; Koike, M.; Miyatake, K.; Watanabe, M. Synthesis and Properties of Anion Conductive Ionomers Containing Fluorenyl Groups for Alkaline Fuel Cell Applications. *Polym. Chem.* **2011**, *2*, 99−106.

(16) Gu, S.; Cai, R.; Yan, Y. S. Self-Crosslinking for Dimensionally Stable and Solvent-Resistant Quaternary Phosphonium Based Hydroxide Exchange Membranes. *Chem. Commun.* **2011**, *47*, 2856−2858.

(17) Li, X.; Yu, Y.; Liu, Q.; Meng, Y. Synthesis and Properties of Anion Conductive Ionomers Containing Tetraphenyl Methane Moieties. *ACS Appl. Mater. Interfaces* **2012**, *4*, 3627−3635.

(18) Zhao, C.; Gong, Y.; Liu, Q.; Zhang, Q.; Zhu, A. Self-Crosslinked Anion Exchange Membranes by Bromination of Benzylmethyl-Containing Poly(sulfone)s for Direct Methanol Fuel Cells. *Int. J. Hydrogen Energy* **2012**, *37*, 11383−11393.

(19) Zhou, J.; Ünlü, M.; Anestis-Richard, I.; Kohl, P. A. Crosslinked, Epoxy-Based Anion Conductive Membranes for Alkaline Membrane Fuel Cells. *J. Membr. Sci.* **2010**, *350*, 286−292.

(20) Abuin, G. C.; Nonjola, P.; Franceschini, E. A.; Izraelevitch, F. H.; Mathe, M. K.; Corti, H. R. Characterization of an Anionic-Exchange Membranes for Direct Methanol Alkaline Fuel Cells. *Int. J. Hydrogen Energy* **2010**, *35*, 5849−5854.

(21) Liu, Z.; Li, X. B.; Shen, K. Z.; Feng, P. J.; Zhang, Y. N.; Xu, X.; Hu, W.; Jiang, Z. H.; Liu, B. J.; Guiver, M. D. Naphthalene-Based Poly(arylene ether ketone) Anion Exchange Membranes. *J. Mater. Chem. A* **2013**, *1*, 6481−6488.

(22) Ma, W.; Zhao, C.; Lin, H.; Zhang, G.; Na, H. Poly(aryl ether ketone)s with Bromomethyl Groups: Synthesis and Quaternary Amination. *J. Appl. Polym. Sci.* **2011**, *120*, 3477−3483.

(23) Rebeck, N. T.; Li, Y.; Knauss, D. M. Poly(phenylene oxide) Copolymer Anion Exchange Membranes. *J. Polym. Sci., Part B: Polym. Phys.* **2013**, *51*, 1770−1778.

(24) Lin, X.; Varcoe, J. R.; Poynton, S. D.; Liang, X.; Ong, A. L.; Ran, J.; Li, Y.; Xu, T. Alkaline Polymer Electrolytes Containing Pendant Dimethylimidazolium Groups for Alkaline Membrane Fuel Cells. *J. Mater. Chem. A* **2013**, *1*, 7262−7269.

(25) Chen, D.; Hickner, M. A. Degradation of Imidazolium- and Quaternary Ammonium-Functionalized Poly(fluorenyl ether ketone sulfone) Anion Exchange Membranes. *ACS Appl. Mater. Interfaces* **2012**, *4*, 5775−5781.

(26) Wang, G.; Weng, Y.; Zhao, J.; Chu, D.; Xie, D.; Chen, R. Developing a Novel Alkaline Anion Exchange Membrane Derived from Poly(ether-imide) for Improved Ionic Conductivity. *Polym. Adv. Technol.* **2010**, *21*, 554−560.

(27) Rao, A. H. N.; Thankamony, R. L.; Kim, H.-J.; Nam, S.; Kim, T.-H. Imidazolium-Functionalized Poly(arylene ether sulfone) Block Copolymer as an Anion Exchange Membrane for Alkaline Fuel Cell. *Polymer* **2013**, *54*, 111−119.

(28) Zhao, Z.; Wang, J.; Li, S.; Zhang, S. Synthesis of Multi-Block Poly(arylene ether sulfone) Copolymer Membrane with Pendant Quaternary Ammonium Groups for Alkaline Fuel Cell. *J. Power Sources* **2011**, *196*, 4445−4450.

(29) Tanaka, M.; Fukasawa, K.; Nishino, E.; Yamaguchi, S.; Yamada, K.; Tanaka, H.; Bae, B.; Miyatake, K.; Watanabe, M. Anion Conductive Block Poly(arylene ether)s: Synthesis, Properties, and Application in Alkaline Fuel Cells. *J. Am. Chem. Soc.* **2011**, *133*, 10646−10654.

(30) Li, N.; Zhang, Q.; Wang, C.; Lee, Y. M.; Guiver, M. D. Phenyltrimethylammonium Functionalized Polysulfone Anion Exchange Membranes. *Macromolecules* **2012**, *45*, 2411−2419.

(31) Lin, B.; Dong, H.; Li, Y.; Si, Z.; Gu, F.; Yan, F. Alkaline Stable C2-Substituted Imidazolium-Based Anion-Exchange Membranes. *Chem. Mater.* **2013**, *25*, 1858−1867.

(32) Qiu, B.; Lin, B.; Si, Z.; Qiu, L.; Chu, F.; Zhao, J.; Yan, F. Bis-Imidazolium-Based Anion-Exchange Membranes for Alkaline Fuel Cells. *J. Power Sources* **2012**, *217*, 329−335.

(33) Kim, D. S.; Labouriau, A.; Guiver, M. D.; Kim, Y. S. Guanidinium-Functionalized Anion Exchange Polymer Electrolytes via Activated Fluorophenyl-Amine Reaction. *Chem. Mater.* **2011**, *23*, 3795−3797.

(34) Zhang, Q.; Li, S.; Zhang, S. A Novel Guanidinium Grafted Poly(aryl ether sulfone) for High-Performance Hydroxide Exchange Membranes. *Chem. Commun.* **2010**, *46*, 7495−7497.

(35) Gu, S.; Cai, R.; Luo, T.; Chen, Z. W.; Sun, M. W.; Liu, Y.; He, G. H.; Yan, Y. S. A Soluble and Highly Conductive Ionomer for High-Performance Hydroxide Exchange Membrane Fuel Cells. *Angew. Chem., Int. Ed.* **2009**, *48*, 6499−6502.

(36) Xu, S.; Zhang, G.; Zhang, Y.; Zhao, C. J.; Zhang, L. Y.; Li, M. Y.; Wang, J.; Zhang, N.; Na, H. Cross-Linked Hydroxide Conductive Membranes with Side Chains for Direct Methanol Fuel Cell Applications. *J. Mater. Chem.* **2012**, *22*, 13295−13302.

(37) Xu, S.; Zhang, G.; Zhang, Y.; Zhao, C. J.; Ma, W. J.; Sun, H. C.; Zhang, N.; Zhang, L. Y.; Jiang, H.; Na, H. Synthesis and Properties of a Novel Side-Chain-Type Hydroxide Exchange Membrane for Direct Methanol Fuel Cells (DMFCs). *J. Power Sources* **2012**, *209*, 228−235.

(38) Shen, K.; Pang, J.; Feng, S.; Wang, Y.; Jiang, Z. Synthesis and Properties of a Novel Poly(aryl ether ketone)s with Quaternary Ammonium Pendant Groups for Anion Exchange Membranes. *J. Membr. Sci.* **2013**, *440*, 20−28.

(39) Zhang, Z.; Wu, L.; Varcoe, J.; Li, C.; Ong, A. L.; Poynton, S.; Xu, T. Aromatic Polyelectrolytes via Polyacylation of Pre-Quaternized Monomers for Alkaline Fuel Cells. *J. Mater. Chem. A* **2013**, *1*, 2595−2601.

(40) Hibbs, M. R.; Fujimoto, C. H.; Cornelius, C. J. Synthesis and Characterization of Poly(phenylene)-Based Anion Exchange Membranes for Alkaline Fuel Cells. *Macromolecules* **2009**, *42*, 8316−8321.

(41) Li, N.; Shin, D. W.; Hwang, D. S.; Lee, Y. M.; Guiver, M. D. Polymer Electrolyte Membranes Derived from New Sulfone Monomers with Pendent Sulfonic Acid Groups. *Macromolecules* **2010**, *43*, 9810−9820.

(42) Pan, J.; Lu, S. F.; Li, Y.; Huang, A. B.; Zhuang, L.; Lu, J. T. High-Performance Alkaline Polymer Electrolyte for Fuel Cell Applications. *Adv. Funct. Mater.* **2010**, *20*, 312−319.

(43) Lin, X.; Wu, L.; Liu, Y.; Ong, A. L.; Poynton, S. D.; Varcoe, J. R.; Xu, T. Alkali Resistant and Conductive Guanidinium-Based Anion-Exchange Membranes for Alkaline Polymer Electrolyte Fuel Cells. *J. Power Sources* **2012**, *217*, 373−380.

(44) Kim, Y. S.; Einsla, B.; Sankir, M.; Harrison, W.; Pivovar, B. S. Structure−Property−Performance Relationships of Sulfonated Poly-(arylene ether sulfone)s as a Polymer Electrolyte for Fuel Cell Applications. *Polymer* **2006**, *47*, 4026−4035.

(45) Lin, B.; Qiu, L.; Qiu, B.; Peng, Y.; Yan, F. A Soluble and Conductive Polyfluorene Ionomer with Pendant Imidazolium Groups for Alkaline Fuel Cell Applications. *Macromolecules* **2011**, *44*, 9642−9649.

(46) Lin, B.; Qiu, L.; Lu, J.; Yan, F. Cross-Linked Alkaline Ionic Liquid-Based Polymer Electrolytes for Alkaline Fuel Cell Applications. *Chem. Mater.* **2010**, *22*, 6718−6725.